392. STUDY OF NATURAL FREQUENCY SHIFTING IN A MEMS ACTUATOR DUE TO VISCOUS AIR DAMPING MODELED BY NONLINEAR REYNOLDS EQUATION

V. Ostasevicius[1], R. Dauksevicius[2], R. Gaidys[3]
[1,2,3] Kaunas University of Technology,
K. Donelaicio 73, LT-44029, Kaunas, Lithuania
E-mail: [1]*vytautas.ostasevicius@ktu.lt*, [2]*rolanasd@centras.lt*, [3]*rimvydas.gaidys@ktu.lt*

(Received 1 August 2008; accepted 10 September 2008)

Abstract: We report on finite element (FE) modeling and simulation of effect of squeeze-film damping on flexible microstructure operating in ambient air in close proximity to a fixed surface, which is a common case in many MEMS devices. A coupled fluidic-structural problem is solved by applying a nonlinear compressible Reynolds equation, which is derived from the Navier-Stokes equations, transformed into weak form and added to commercial FE modeling software. The proposed model enables investigation of influence of surrounding air on dynamics of different microstructures taking into account air rarefaction and air compressibility effects. The paper presents results of numerical analysis, which aim was to study the phenomenon of natural frequency shifting in the case of free and forced vibrations of the cantilever microstructure. Simulations demonstrate that squeeze-film damping may result in the increase of natural frequency of the microstructure due to system stiffening caused by air compression. The magnitude of this effect is determined by such parameters as ambient air pressure, air-film thickness, vibration frequency and lateral dimensions of the microstructure.

Keywords: MEMS, squeeze-film damping, finite element modeling, nonlinear compressible Reynolds equation, natural frequency shift, stiffening.

Introduction

Squeeze-film damping is characteristic for devices of microelectromechanical systems (MEMS) which design is based on parallel-plate capacitor structures, in which air fills tiny gap between two parallel plates (e.g. vertical microaccelerometers, torsional micromirrors or micro-switches)(Fig. 1). In order to increase the efficiency of actuation (for microactuators) or improve the sensitivity of capacitive detection (for microsensors), the distance between the capacitor plates is minimized and the area of the plates is maximized. When in operation, vibrating microstructure of such MEMS devices is undergoing transverse motion with respect to substrate. Since the lateral dimensions of the microstructure are much larger than the gap size, its fairly small displacement in normal direction compresses (or pulls back) a significant amount of air out of (or into) the very narrow gap. However, the viscosity of the air film limits the flow rate along the gap, and thus the pressure is increased inside the gap and acts against the microstructure. The total pressure force, which opposes the motion of the microstructure, is known as squeeze-film damping. It strongly affects the dynamic behavior of microdevices. The reason of this strong influence is the scaling effect: volume forces (such as gravity and inertia) that act on a device are directly proportional to the $(\text{length})^3$, while surface forces (such as viscous force) are proportional to the $(\text{length})^2$, thus, the effect of surface forces on microdevices is relatively greater than the effect of volume forces. And since the damping force of the surrounding air is a surface force, it plays an important role in microdevices, whereas it can be neglected for machines of macroscopic dimensions [1-5]. Squeezed gas effects were studied long before advent of MEMS. Major applications of this effect were related to bearings (lubrication), levitation systems and dampers for pneumatic machines [6-8]. History of research on air damping in MEMS was started by W.E. Newell in 1968 just after the first MEMS device was developed by H.C. Nathanson in 1967. Newell discussed the influence of surrounding air on the quality factor of a resonator and he observed that the ever-present damping due to the ambient air would be increased when the resonator was near a second surface due to the pumping action of the air

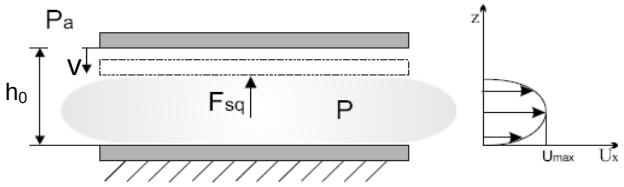

Fig. 1. Graphical representation of squeeze-film damping between two parallel plates that move normal to each other and velocity profile of the generated gas flow. *P* – pressure between plates, P_a – ambient pressure, *U* – gas flow velocity, *v* – plate velocity, F_{sq} – squeezed film force, h_0 – initial gas film thickness.

between the surfaces. Later, in 1983 J. Blech analyzed squeeze-film damping and discussed application of this effect to tailor frequency response of seismic accelerometers. Extensive research of air damping in MEMS started at the end of 80s - beginning of 90s (H.V. Allen, H. Seidel, J.B. Starr [9], M. Andrews [10], H. Tilmans [11], T. Veijola [12] etc.) [1-5].

Mathematical models of different dimensionality and complexity have been used by numerous researchers to help understand and characterize MEMS structures under the influence of squeeze-film damping. Reynolds equation known from lubrication technology is the theoretical background to analyze this phenomenon. Much of theoretical research work on squeeze-film damping in MEMS by using Reynolds equation treats vibrating microstructures as rigid, i.e. lumped spring-mass (single degree-of-freedom) models are utilized [9,10,14-17]. A number of researchers use models that account for flexibility of microstructures and treat them as distributed-parameter systems [18-22], however many of them use simplified versions of Reynolds equation [18,20,21]. All models are almost exclusively based on linearized Reynolds equation [10,15,16,21] or its simplest version – linearized incompressible Reynolds equation [9,12,17,18,20]. Those models that use nonlinear Reynolds equation, however, have a tendency to approximate a microstructure by a beam model [19,23]. Thus, we may conclude that those models that account for flexibility of microstructures either simplify the structural problem (as in [19,23]) or the squeeze-film damping problem (as in [18,20,21]).

The presented literature review suggests that there is a need for accurate computational models that represent microstructure in 3-D, account for its flexibility by treating it as a distributed-parameter system, and are suitable for dynamic analysis of influence of forces generated by surrounding gas environment From the analysis point of view, it is important to determine how different squeeze-film damping conditions influence dynamic behavior of the microsystem.

Derivation of Reynolds equation

On the continuous field level, squeeze-film damping of a microstructure vibrating in a fluid is governed by

Table 1. List of proposed expressions for effective viscosity coefficient μ_{eff}. The parameter α is the accommodation coefficient, defined by interaction between the surfaces and the gas (for most engineering surfaces it can be assumed to be equal to unity) and *Q* is Poiseuille flow rate [12].

Author (year)	Expression for μ_{eff}
Knudsen (1906)	$\frac{\mu}{1+\frac{K_n(K_n+2.507)}{0.1474(K_n+3.095)}}$
Burgdorfer (1959)	$\frac{\mu}{1+6K_n}$
Hsia and Domoto (1983)	$\frac{\mu}{1+6K_n+6K_n^2}$
Fukui and Kaneko (1988)	$\frac{\mu D}{6Q(D)}, D=\frac{\sqrt{\pi}}{2K_n}$
Seidel et al. (1993)	$\frac{0.7\mu}{0.7+K_n}$
Mitsuya (1993)	$\frac{\mu}{1+6\frac{2-\alpha}{\alpha}K_n+\frac{8}{3}K_n^2}$
Veijola et al. (1995)	$\frac{\mu}{1+9.638K_n^{1.159}}$

Navier-Stokes (NS) equations, which are composed of the continuity equation and the motion equation:

$$\frac{\mathrm{D}\rho}{\mathrm{D}t}+\rho\ \nabla\mathbf{U},$$
$$\frac{\mathrm{D}\rho}{\mathrm{D}t}=-\nabla P+\rho\ g+\eta\nabla^2\mathbf{U}+\frac{\eta}{3}\nabla(\nabla\times\mathbf{U}). \quad (1)$$

where ρ is density of the fluid, η is the absolute viscosity (assumed to be constant), *g* is the acceleration of gravity, *P* is the pressure of the fluid and **U** is the velocity of the fluid (bold symbol denotes vector quantity) [5].

NS equations are very difficult to solve analytically and exact solutions only can be found for problems with one dependent variable. In most cases these partial differential equations are solved using computational fluid dynamics techniques that are one of the most challenging tasks for FE solvers. In contrast to structural mechanics or thermal analysis, solution must be done iteratively. Solution requires relatively more equilibrium iterations and strong convergence problems occur frequently.

Furthermore, if we wanted to include contact model into the model based NS equations, the computational effort required for dynamic simulations using such complicated model would be enormous and hardly possible with current stand-alone computers. The most

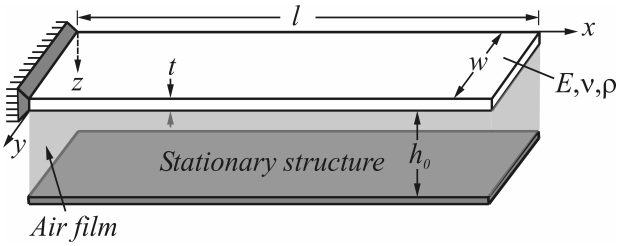

Fig. 2. Schematic of the modeled fluidic-structural microsystem consisting of a cantilever microstructure under the effect of forces generated by squeezed air film.

common method to avoid usage of NS equations for modeling squeeze-film damping in MEMS is to apply Reynolds equation, which is used in lubrication theory to determine the behavior of a thin fluid film between two moving surfaces [6]:

$$\frac{\partial}{\partial x}\left(\frac{\rho h^3}{\mu}\frac{\partial P}{\partial x}\right)+\frac{\partial}{\partial y}\left(\frac{\rho h^3}{\mu}\frac{\partial P}{\partial y}\right)= \\ =6\left\{2\frac{\partial(\rho h)}{\partial t}+\frac{\partial}{\partial x}\left[\rho h(u_1+u_2)\right]+\frac{\partial}{\partial y}\left[\rho h(v_1+v_2)\right]\right\}. \quad (2)$$

where fluid density ρ, pressure in the gap P, and the gap thickness h are functions of time and position (x, y). μ is the dynamic viscosity of the fluid, u_1 and u_2 are the velocities in the x-direction of the top and the bottom surface, respectively, and v_1 and v_2 are the velocities in the y-direction of the two surfaces.

Reynolds equation is a nonlinear partial differential equation, which is derived from Navier-Stokes equation, the equation for the conservation of mass and the equation of state for an ideal gas by assuming that (1) the fluid is Newtonian (the shear stress is directly proportional to the velocity), (2) the fluid obeys the ideal gas law, (3) the inertia and body forces are negligible compared to the viscous and pressure forces, (4) the variation of pressure across the fluid film is negligibly small, (5) the flow is laminar, (6) the thickness of fluid film is very small compared to the lateral dimensions of the moving and stationary plates, (7) the fluid is treated as continuum and does not slip at the boundaries [1,4,6].

The condition of negligible inertia effect of fluid is written by using the following condition for modified Reynolds number [13]:

$$\frac{\omega h^2 \rho}{\mu} << 1. \quad (3)$$

where, ω is angular oscillation frequency of the moving structure.

Since the relative movement in lateral direction is not considered for MEMS devices, the original Reynolds equation is reduced to:

Table 2. Parameters of modeled fluidic-structural microsystem.

Description and Symbol	Value	Unit
Microstructure length l	117	[μm]
Microstructure width w	30	[μm]
Microstructure thickness t	2.0	[μm]
Initial air-film thickness h_0	2.0	[μm]
Young's modulus E	207	[GPa]
Density ρ	8908	[kg/m^3]
Poisson's ratio ν	0.31	-
Dynamic viscosity of air μ	18.3×10^{-6}	[Pa s]

$$\frac{\partial}{\partial x}\left(\frac{\rho h^3}{\mu}\frac{\partial P}{\partial x}\right)+\frac{\partial}{\partial y}\left(\frac{\rho h^3}{\mu}\frac{\partial P}{\partial y}\right)=12\frac{\partial(\rho h)}{\partial t}. \quad (4)$$

Gas is a predominant working fluid in MEMS devices and thin gas films are realistically assumed to be isothermal, i.e. it is assumed that viscous friction does not cause a significant temperature change since: (a) thermal contact between the gas and the surrounding solid surfaces is very good in MEMS devices (volumes are small and surface areas are large), and (b) common MEMS materials are good thermal conductors [1]. The equation of state for an ideal gas is [6]:

$$\frac{P}{\rho}=\overline{R}t_g. \quad (5)$$

where $\overline{R}$ – specific gas constant (universal gas constant/molar mass), t_g – gas temperature.

For isothermal process P/ρ is constant and therefore density in the Reynolds equation can be replaced with pressure [6]. The equation given below is known as isothermal compressible Reynolds equation, which will be further referred to as nonlinear Reynolds equation (NRE):

$$\frac{\partial}{\partial x}\left(\frac{Ph^3}{\mu}\frac{\partial P}{\partial x}\right)+\frac{\partial}{\partial y}\left(\frac{Ph^3}{\mu}\frac{\partial P}{\partial y}\right)=12\left(h\frac{\partial P}{\partial t}+P\frac{\partial h}{\partial t}\right). \quad (6)$$

where total pressure $P(x,y,t)=p_0+\overline{P}(x,y,t)$, p_0 is the initial static ambient pressure in the gap and $\overline{P}(x,y,t)$ is the deviatory (additional) pressure caused by the squeezed air-film effect.

Reynolds equation assumes continuous fluid flow regime. A general condition of acceptance of this assumption is the Knudsen number K_n, which is a measure of the viscosity of the gas under the microstructure [2]:

$$K_n=\frac{L_0 P_{atm}}{p_0 h_0}. \quad (7)$$

where h_0 – initial value of gap (gas film) thickness, L_0 is the mean free path of air particles at atmospheric pressure P_{atm} (i.e. the distance covered by a molecule in a

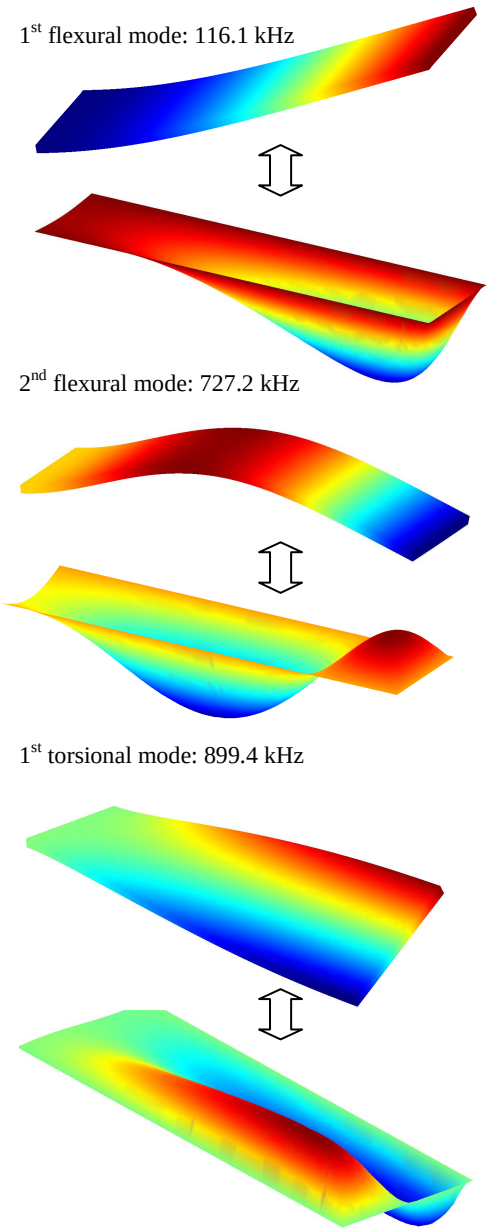

Fig. 3. Simulation results: vibration mode shapes of cantilever microstructure and the corresponding pressure mode shapes.

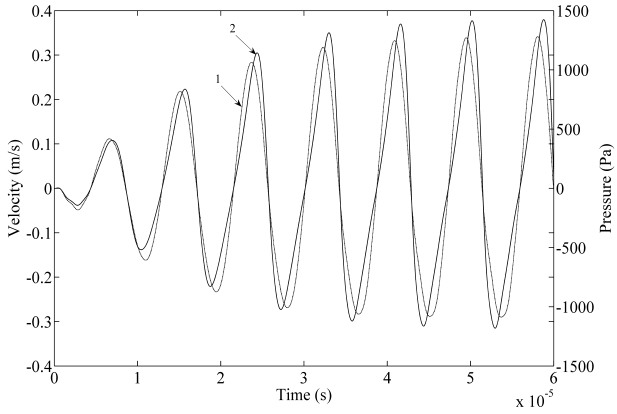

Fig. 4. Time responses of velocity (1) and pressure (2) at arbitrary midpoint of cantilever microstructure excited with sinusoidal force of the magnitude that produces large-amplitude vibrations and which frequency is equal to fundamental frequency of microstructure in the presence of squeeze-film damping.

gas between successive collisions). For the P_{atm} = 101325 Pa, $L_0 \approx 65$ nm [1]. Based on the Knudsen number, the flow can be divided into four regimes: continuum flow (when $K_n < 0.001$), slip flow (when $0.001 < K_n < 0.1$), transitional flow (when $0.1 < K_n < 10$), and free molecular flow when ($K_n > 10$) [1]. In the continuum regime, the fluid is governed by the Navier-Stokes equations (or equivalently the Reynolds equation). However, many MEMS devices are designed to operate at very low pressure with a very small gap between the electrodes. Under such rarefied gas conditions, Knudsen number increases to the noncontinuum regimes and interaction of gas molecules with the surfaces become important, reducing gas viscosity, through so-called "slip effect" where particles can have fewer interactions before escaping [1,5]. Thus, the use of original Reynolds equation in the noncontinuum regimes is not correct. Fortunately, extensive research has extended the validity of Reynolds equation to the noncontinuum regimes, thereby enabling description of the flow using single model. A convenient and popular way to account for gas rarefaction effects is to modify dynamic viscosity μ in Reynolds equation by introducing effective viscosity coefficient μ_{eff}. Various expressions have been proposed by different researchers for μ_{eff} since the beginning of the 20th century, when Knudsen presented a correction coefficient based on his research on the gas flow in capillary tubes [12]. Summary of these expressions is given in Table 1. Though all expressions give similar results, expression from Veijola et al. is valid over a wider range of K_n in comparison to others ($0 \le K_n \le 880$) and therefore is widely used in squeeze-film damping analysis [2,12,13].

3. Formulation of a model of the fluidic-structural microsystem

A microstructure having cantilever-type or fixed-fixed configuration is a basic structural element of most MEMS actuators and sensors such as microswitches, capacitive pressure sensors, accelerometers, filters, resonators and many others. Schematic drawing of a basic modeled fluidic-structural microsystem with typical parameter values are provided in Fig. 2. Firstly, a mechanical model of the microstructure was created in the finite element (FE) modeling software Comsol [13]. In the FE formulation microstructure dynamics is described by the following equation of motion presented in a general matrix form:

$$[M]\{\ddot{U}\}+[C]\{\dot{U}\}+[K]\{U\}=\{Q(t,U,\dot{U})\}. \quad (8)$$

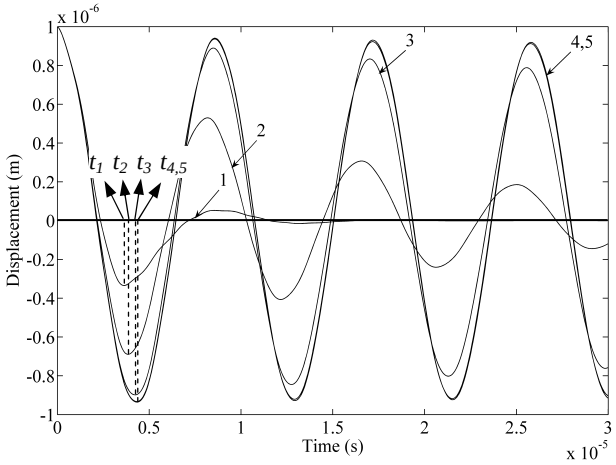

Fig. 5. Simulated free vibration response curves of the arbitrary point at the end of the microstructure after it was released from its initial deflected position z_0 = 1 μm for different p_0 in the gap of h_0 = 1 μm. Curves: 1– 10^5 Pa, 2 – 10^4 Pa, 3 – 10^3 Pa, 4 – 10^2 Pa, 5 – 10 Pa.

where $[M],[C],[K]$ are mass, damping and stiffness matrices respectively, $\{U\},\{\dot{U}\},\{\ddot{U}\}$ – displacement, velocity and acceleration vectors, $\{Q(t,U,\dot{U})\}$ – vector representing air pressure forces generated by fluidic-structural interaction between the microstructure and ambient air.

The model consists of a flexible 3D microstructure, which is fixed at x = 0 and is suspended by distance h_0 over a stationary structure. Parameters listed in the table of Fig. 2 are used for simulations. It is assumed that both structures are surrounded by the air. Therefore the gap in-between is filled by the air and forms an air-film, which is characterized by the following parameters that are specified in Comsol during pre-processing stage: h_0 – initial air-film thickness, μ – dynamic viscosity of air at standard pressure and temperature STP (101 kPa, 25°C), L_0 – mean free path of air particles at atmospheric pressure and p_0 – initial ambient pressure. The microstructure is initially at rest in its undeformed configuration.

In order to add the effect of squeeze-film damping to the mechanical model, it was necessary to transform eq. 6 into weak form and insert into the Comsol. To this end the procedure provided below was performed.

The variable gap thickness h is expressed as:

$$h(x,y,t) = h_0 - z(x,t)\ . \tag{9}$$

where $z(x,t)$ is deflection of the microstructure.

Then we obtain the following form of compressible Reynolds equation by taking into account that $P(x,y,t) = p_0 + \overline{P}(x,y,t)$ and $\mu = \mu_{eff}$ (model of Veijola is used here for μ_{eff} as given in Table 1):

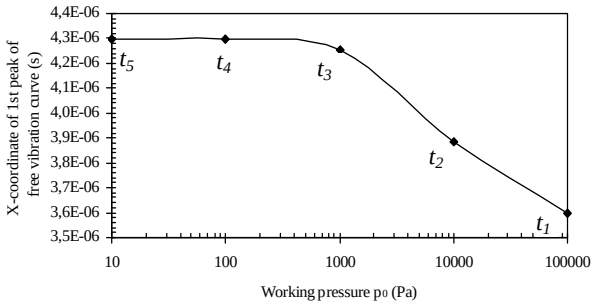

Fig. 6. Variation of time-coordinate of peaks of free vibration response curves corresponding to different values of working pressure p_0 as indicated in Fig. 5 with t_1, t_2, t_3, t_4 and t_5.

$$\frac{\partial}{\partial x}\left[(h_0-z)^3 p_0 \frac{\partial \overline{P}}{\partial x}\right] + \frac{\partial}{\partial y}\left[(h_0-z)^3 p_0 \frac{\partial \overline{P}}{\partial y}\right] = 12\mu_{eff}\left[(h_0-z)\frac{\partial \overline{P}}{\partial t} - p_0 \frac{\partial z}{\partial t}\right]. \tag{10}$$

Air can freely move into and out of the gap. The additional time-dependent pressure component $\overline{P}(x,y,t)$ appears due to transient changes in the gap size during microstructure movement and it depends on the gap size and its deformation velocity as well as on the properties of the air and the structures. Because the system's surroundings are in equilibrium, the only force component that affects the moving microstructure results from the additional film pressure $\overline{P}(x,y,t)$.

Dirichlet boundary condition is:

$$\overline{P}(0,y,t) = p_0\ . \tag{11}$$

Neuman boundary conditions are:

$$\frac{\partial \overline{P}(l,y,t)}{\partial x} = 0\ , \tag{12}$$

$$\frac{\partial \overline{P}(x,0,t)}{\partial x} = 0\ , \tag{13}$$

Due to symmetry only half of the microstructure is modeled therefore the condition at symmetry is as follows:

$$\frac{\partial \overline{P}(x,w/2,t)}{\partial n} = 0\ . \tag{14}$$

where, **n** – outward normal vector.

At open edges of the microstructure the pressure is equal to p_0, i.e. variation of $\overline{P}(x,y,t)$ vanishes at the edges of the gap. This is an adequate assumption since the aspect ratio (ratio between lateral dimensions and

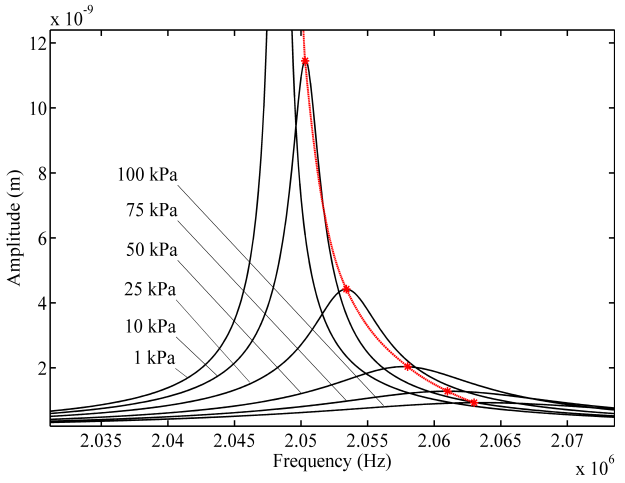

(a)

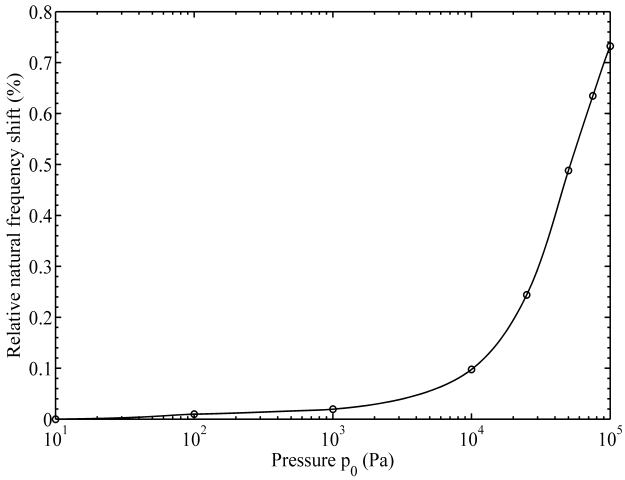

(b)

Fig. 7. Simulation results: (a) amplitude-frequency characteristics of arbitrary point of the microstructure in the vicinity of its 3rd natural frequency and in the presence of squeeze-film damping at different levels of working pressure p_0. (b) Relative shift of 3rd natural frequency of the microstructure presented as a function of working pressure p_0, (h_0 = 1 μm, l = 117 μm, f_3 = 2.0482 MHz, σ = 16.1 at $p_0 = P_{atm}$).

thickness of the air-film) of the considered microsystem is large.

Then eq. 10 is multiplied by some test function V and integrated over the domain of interest denoted by Ω:

$$\int_\Omega \left[\frac{\partial}{\partial x}\left[(h_0 - z)^3 p_0 \frac{\partial \overline{P}}{\partial x} \right] V + \frac{\partial}{\partial y}\left[(h_0 - z)^3 p_0 \frac{\partial \overline{P}}{\partial y} \right] V \right] d\Omega = $$
$$= 12\mu_{eff} \int_\Omega \left[(h_0 - z)\frac{\partial \overline{P}}{\partial t} - p_0 \frac{\partial z}{\partial t} \right] V \, d\Omega. \quad (15)$$

Applying the Green-Gauss theorem and integrating by parts we obtain the following relation:

$$\int_\Omega \left[\left[\left((h_0 - z)^3 p_0 \frac{\partial \overline{P}}{\partial x} \right) \frac{\partial V}{\partial x} + \left((h_0 - z)^3 p_0 \frac{\partial \overline{P}}{\partial y} \right) \right] \frac{\partial V}{\partial y} \right] d\Omega -$$
$$- \int_{\partial\Omega} \vec{n}_x \left[\left((h_0 - z)^3 p_0 \frac{\partial \overline{P}}{\partial x} \right) V + \vec{n}_y \left((h_0 - z)^3 p_0 \frac{\partial \overline{P}}{\partial y} \right) V \right] dS =$$
$$= \int_\Omega 12\mu_{eff} \left[V(h_0 - z)\frac{\partial \overline{P}}{\partial t} - V p_0 \frac{\partial z}{\partial t} \right] d\Omega. \quad (16)$$

where $\partial\Omega$ denotes the boundary on the domain Ω.

Taking into account boundary conditions we get the weak form of eq. 10:

$$\int_\Omega \left[\left((h_0 - z)^3 p_0 \left(\frac{\partial \overline{P}}{\partial x}\frac{\partial V}{\partial x} + \frac{\partial \overline{P}}{\partial y}\frac{\partial V}{\partial Y} \right) - \right.$$
$$\left. - 12\mu_{eff} \left(V(h_0 - z)\frac{\partial \overline{P}}{\partial t} - V p_0 \frac{\partial z}{\partial t} \right) \right] d\Omega = 0. \quad (17)$$

The obtained weak formulation of the compressible Reynolds equation was inserted into the Comsol FE model and "coupled" to a lower surface (boundary) of the microstructure. It was possible to perform this insertion of weak form of Reynolds equation into the Comsol due to the unique feature of the software, referred to as "equation-based modeling", which enables the user to input any number of equations via graphical user interface. When the equation is inserted, the software uses a special equation interpreter to automatically translate the expression into a finite element code. Thereby Comsol solves entered Reynolds equations in order to determine pressure distribution in the gap and then this pressure acts as a boundary load on the microstructure. The developed FE model was subsequently used for numerical study of squeezed-film effects.

3. Simulation results

Numerical analysis of squeeze-film damping starts with modal analysis, which purpose is to determine the distribution of air pressure forces in the gap when cantilever microstructure is vibrating in its flexural and torsional resonant modes. Comsol eigenfrequency solver is used for the simulations. Ambient pressure p_0 in the gap is set to atmospheric value of P_{atm} = 101 kPa. For better visualization model symmetry is not used here. The results, presented in Fig. 3, consist of several natural frequencies of the microstructure, corresponding structural mode shapes and the associated pressure mode shapes. When examining these results we may notice the obvious coupling between structural displacements of the microstructure and the pressure distribution in the gap. For example, in the 2nd flexural mode, the upward flexing of middle part of microstructure corresponds to a concave pressure profile in the respective region of

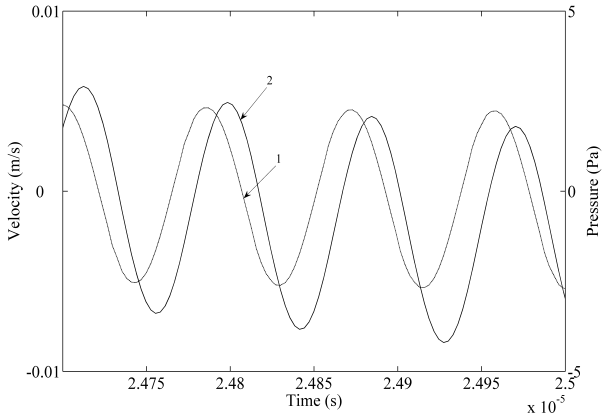

Fig. 8. Simulation results: comparison of responses of velocity (1) and pressure (2) at arbitrary midpoint at the free end of cantilever microstructure excited with sinusoidal force of the magnitude that produces small-amplitude vibrations and which excitation frequency f_e equals to $100f_1$.

pressure distribution plot, which indicates the reduction of pressure in this part of the gap (i.e. decompression effect). And, in contrast, the downward flexing of free end of the microstructure corresponds to a convex pressure profile – zone of increased pressure with respect to atmospheric (i.e. compression effect).

Simulations of forced vibrations of microstructure were carried out by exciting lower edge of the free end of the microstructure with a sinusoidal force:

$$F_e = F_a \sin(2\pi f_e t). \tag{18}$$

where f_e – excitation frequency, F_a – excitation force amplitude.

Fig. 4 presents transient responses of velocity and pressure at arbitrary midpoint at the free end of cantilever microstructure excited with sinusoidal force of the magnitude that produces large-amplitude vibrations in the presence of squeeze-film damping. Large-amplitude vibrations (with respect to air-film thickness h_0) are achieved when excitation force generates displacement of free end of the microstructure that is equal or close to h_0. Fig. 4 indicates a nonlinear pressure response with respect to velocity response.

In order to determine influence of squeeze-film damping effects on free vibrations of the microstructure, the latter is set to oscillate freely by displacing upwards its lower edge at the free end by a certain distance z_0 (static analysis) and then releasing (transient analysis). Large-amplitude free vibrations were obtained by selecting value of z_0 such that $h_0/z_0 \approx 1$. The results of this numerical analysis are provided in Fig. 5. By observing the time-coordinate of amplitude peaks of curves corresponding to different levels of p_0 (t_1, t_2, t_3, t_4, t_5) it is possible to notice that the time-coordinate of the peak decreases (from t_5 to t_1) with increase in p_0. Fig. 6 illustrates the variation of time-coordinate of the peaks with respect to ambient pressure p_0 represented on logarithmic scale. It is obvious that the most pronounced reduction is from t_3 to t_1 as p_0 changes from 1 kPa to 100 kPa. Total relative decrease from t_5 to t_1 is 16.3 %. This effect also manifests in the case of small-amplitude ($h_0/z_0 \approx 100$) free vibrations but in this case it is not so significant. Reduction of time-coordinate of amplitude peak with increasing pressure indicates that the frequency of natural vibrations increases and this in turn implies that in this case air undergoes compression leading to natural frequency shift. This agrees with the known fact that in the case of squeeze-film damping phenomenon pressure force exerted by the air-film undergoing periodic cycles of compression and decompression has two components: one is in phase with the microstructure velocity (i.e. viscous damping force) and the other is in phase with the displacement (i.e. elastic force component due to compressibility of air). A non-dimensional squeeze number σ is used to characterize the degree of compression of the air in the gap [4]:

$$\sigma = \frac{12\mu_{eff} L^2 \omega}{p_0 h_0^2}. \tag{19}$$

where L is the characteristic length – the shortest lateral dimension of the microstructure, ω – angular oscillation frequency of the microstructure.

At relatively low oscillation frequencies ω or relatively large air gaps h_0 (i.e. low squeeze number – roughly $\sigma \leq 3$ [2]), the viscous damping force dominates because the air can escape out of the gap without being compressed. While, at relatively high ω or relatively small h_0 (i.e. high σ), elastic forces increase because of the air-film compression effect. In practice, the squeezed air-film represents a combination of viscous damping and elastic forces [4]. The main effect of air compression at high values of σ is the stiffening of the microsystem, which consequently increases its natural frequency.

A sequence of frequency response analyses was carried out by applying harmonic load (eq. 18) in order to study the phenomenon of natural frequency shifting. The condition of larger σ was achieved by increasing excitation frequencies f_e and therefore the simulation was performed in the vicinity of 3rd natural frequency of transverse vibrations of analyzed microstructure (f_3 = 2.05 MHz). The squeeze number for this case was equal to σ = 16.1 at $p_0 = P_{atm}$. Obtained amplitude-frequency characteristics, provided in Fig. 7(a), clearly demonstrate that air undergoes compression and this in turn raises the natural frequency of the microstructure as the pressure increases from 1 kPa to 100 kPa. Fig. 7(b) illustrates the change of relative frequency shift as a function of p_0. Simulation results reveal that the 3rd natural frequency of transverse vibrations in air at $p_0 = P_{atm}$ is by 0.73 % higher than the value obtained under vacuum conditions (p_0 = 0). It should be pointed out that no significant pressure dependence was observed below 100 Pa and this result is in agreement with experimental results and observations found in open literature [11].

Another sequence of transient simulations was carried out during which free end of cantilever microstructure was excited with sinusoidal force of the amplitude that produces small-amplitude vibrations and which frequency f_e is 100 times larger than the first natural frequency of the microstructure f_1. Fig. 8 demonstrates obtained transient responses of velocity (curve 1) and pressure (curve 2) at arbitrary midpoint at the free end of cantilever microstructure. The figure clearly indicates that the pressure lags behind the sinusoidal velocity. Simulations revealed that the magnitude of the phase lag increases with vibration frequency. This in turn indicates that increase in vibration frequency changes the character of squeeze-film damping phenomenon by lowering viscous damping forces and raising elastic forces.

Conclusion

Results of modeling and simulation of squeeze-film damping phenomenon in the case of cantilever-type fluidic-structural microsystem were presented in the paper. The developed finite element model is suitable for numerical analysis of the coupled fluidic-structural problem in the case of flexible microstructure operating in ambient air in close proximity to a fixed surface, which is a common case in different MEMS sensors and actuators such as microswitches, capacitive pressure sensors, accelerometers, filters, resonators, etc. The model enables evaluation of influence of surrounding air on the dynamic characteristics of the microstructures. Proposed model accounts for air rarefaction effects and is valid in wide a pressure range of 10 Pa ÷ 100 kPa. The particular emphasis of performed numerical analysis was on study of air compressibility effects leading to system stiffening, which results in the increase of natural frequency of the microstructure in comparison to results obtained under vacuum conditions.

For modeling of squeeze-film damping a nonlinear compressible isothermal Reynolds equation was used. It was derived from the Navier-Stokes equations, subsequently transformed into weak formulation and inserted into mechanical finite element model of the cantilever microstructure, developed with the Comsol software, thereby expanding the capabilities of the software to perform more in-depth study of the considered squeeze-film damping phenomenon.

Numerical modal analysis was performed, which provided natural frequencies and mode shapes of a microstructure together with the corresponding pressure distribution in the gap.

Simulations performed in the case of large-amplitude motion of the microstructure demonstrated the nonlinear response of the pressure in the air-film with respect to velocity response of the microstructure.

Effect of natural frequency shifting was analyzed and observed in the case of free and forced vibrations of the microstructure. It was confirmed that vibration frequency of the microstructure changes the character of squeeze-film damping phenomenon by reducing generated viscous air damping forces and increasing elastic forces. It is concluded that natural frequency shifting is observed under specific operating conditions that are defined by a combination of values of ambient pressure, air-film thickness, vibration frequency and lateral dimensions of the microstructure.

References

[1] **Gad-el-Hak M.** The MEMS Handbook, CRC Press, USA, 2002.

[2] **Rebeiz G.B.** RF MEMS: Theory, Design, and Technology, Wiley-Interscience, USA, 2003.

[3] **Lin R.M., Wang W.J.** Structural Dynamics of Microsystems - Current State of Research and Future Directions. Mechanical Systems and Signal Processing, Vol. 20, pp. 1015-1043, 2006.

[4] **Senturia S.D.** Microsystem Design. Kluwer Academic Publishers, Norwell, USA, 720 p., 2001.

[5] **Pelesko J.A., Bernstein D.H.** Modeling MEMS and NEMS. Chapman Hall and CRC Press, Boca Raton, USA, 384 p., 2003.

[6] **Hamrock B.J., Schmid S.R., Jacobson B.O.** Fundamentals of Fluid Film Lubrication. Marcel Dekker Inc., New York, USA, 672 p., 2004.

[7] **Griffin W.S., Richardson H.H., Yamanami S.A.** Study of Fluid Squeeze-Film Damping. Journal of Basic Engineering, Transactions of ASME, Vol. 88, pp. 451-456, 1966.

[8] **Shadd M.H., Stiffler A.K.** Squeeze Film Dampers: Amplitude Effects at Low Squeeze Numbers. Journal of Engineering for Industry, Transactions of the ASME, Vol. 57, pp. 1366-1370, 1975.

[9] **Starr J.B.** Squeeze-Film Damping in Solid-State Accelerometers, Proc. of the IEEE Solid-State Sensor and Actuator Workshop, Hilton Head Island, USA, pp. 44-47, June 1990.

[10] **Andrews M., Harris I, Turner G.** A Comparison of Squeeze-Film Theory With Measurements on a Microstructure. Sensors and Actuators A, Vol. 36, pp. 79-87, 1993.

[11] **Tilmans H.A.C., Legtenberg R.** Electrostatically Driven Vacuum-Encapsulated Polysilicon Resonators (part I & II). Sensors and Actuators A, Vol. 45, pp. 67-84, 1994.

[12] **Veijola T., Kuisma H., Lahdenpera J., Ryhanen T.** Equivalent Circuit Model of the Squeezed Gas Film in a Silicon Accelerometer. Sensors and Actuators A, Vol. 48, pp. 239-248, 1995.

[13] Comsol Multiphysics 3.2 software user manual, 2005.

[14] **Bao M., Yang H., Sun Y., French P.J.** Modified Reynolds' Equation and Analytical Analysis of Squeeze-Film Air Damping of Perforated Structures. Journal of Microemechanics and Microengineering, Vol. 13, pp. 795-800, 2003.

[15] **Darling R.B., Hivick C., Xu J.** Compact Analytical Modeling of Squeeze Film Damping with Arbitrary Venting Conditions Using a Green's Function Approach. Sensors and Actuators A, Vol. 70, pp. 32-41, 1998.

[16] **Zhang W.-M. Meng G., Li H.-G.** Modeling and Simulation of the Squeeze Film Effect on the MEMS structures. Proc. of Asia-Pacific Microwave Conference, Suzhou, China, Vol. 2, pp. 1-3, December 2005.

[17] **Chu P.B., Nelson P.R., Tachiki M.L., Pister K.S.** Dynamics of Polysilicon Parallel-Plate Electrostatic

Actuators. Sensors and Actuators A, Vol. 52, pp. 216-220, 1996.

[18] Decuzzi P., Demelio G.P., Pascazio G., Zaza V. Bouncing Dynamics of Resistive Microswitches With an Adhesive Tip. Journal of Applied Physics, Vol. 100, pp. 1-9, 2006.

[19] McCarthy B., Adams G.G., McGruer N.E., Potter D. A Dynamic Model, Including Contact Bounce, of an Electrostatically Actuated Microswitch. Journal of Microelectromechanical Systems, Vol. 11, pp. 276-283, 2002.

[20] Eriksson A. Mechanical Model of Electrostatically Actuated Shunt Switch. Proc. of Comsol User Conference, pp. 1-6, 2005.

[21] Schauwecker B., Mehner J., Luy J.-F. Modeling and Simulation Considerations for a New Micro-Electro-Mechanical Switch - Toggle Switch. Proc. of Silicon Monolithic Integrated Circuits in RF Systems, Grainau, Germany, pp. 192-195, April 2003.

[22] Nayfeh A.H., Younis M.I. A New Approach to the Modeling and Simulation of Flexible Microstructures under the Effect of Squeeze-Film Damping. Journal of Microemechanics and Microengineering, Vol. 14, pp. 170-181, 2004.

[23] Hung E.S., Senturia S.D. Generating Efficient Dynamical Models for Micro-Electromechanical Systems From a Few Finite-Element Simulations Runs. Journal of Microelectromechanical Systems, Vol. 8, pp. 280-289, 1999.